Analysis of 3 kV DC Contact Line High-Speed Circuit Breaker Unit Protection Scheme Limitations

Wonder Mukwata and Josiah Munda
Department of Electrical Engineering, Tshwane University of Technology, Pretoria, 0001, South Africa
Email: wondermukwata@yahoo.com, mundajl@tut.ac.za

***Abstract*—The High-Speed Circuit Breaker (HSCB) is a de-facto electro-mechanical contact line protection device employed in the 3 kV DC traction power supply system. The breakers installed at the terminal ends of the contact line make a unit protection scheme configuration. While the HSCBs seem to trip under fault conditions, there is an unknown source that keeps on supplying residual current into the faults. This necessitates some explanation of the source of energy of the continual flow of residual energy. This paper makes an analysis of the limitations in the HSCB unit protection scheme using MATLAB simulation and how the scheme can be optimized with digital protection devices augmented with a peer-to-peer transfer trip as an end-to-end protection solution.**

***Index Terms*—unit protection scheme, residual current, residual energy, digital protection relays, peer-to-peer transfer trip**

I. Introduction

The high-speed circuit breaker (HSCB) is a critical subsystem element of a railway electrification system. The HSCB is the electrical interface between the traction substation and the 3 kV DC overhead contact line providing the fundamental element for primary protection. The system functions in a substantially different condition from the static nature of A.C. power plants in that the loads in the form of electrical multiple units (EMUs) are dynamic. This characteristic is a determinant for discrete protection for the contact line's electrical loading that is not constant but dependent on time variable current loading of moving EMUs. The loading feature made by the overlapping currents expended by the EMUs and under fault conditions determines the difference.

An HSCB unit protection scheme is employed in double-fed contact line systems that use breakers at their terminal ends with the same protection settings to detect faults. Where faults occur, the breakers trip independently. The breaker that is closer to the overload or fault trips while the one that is at the remote end does not trip or takes time to trip. Under these conditions, the breaker that does not trip or delays in tripping keeps supplying residual energy into the fault. This paper makes an analysis with options to improve the limitations by appropriating protection solutions based on open standards with a protection and control scheme. Based on a conception where it is controlled by autonomous protection and control units in compliance with the requirements for a transfer tripping system requirement, this can guarantee that a fault on a contact line can be sensed from the in-feed points independently.

Nomenclature

s	Distance between substation
Δs	Incremental step change in distance
V_a	Substation A bus voltage
V_b	Substation B bus voltage
I	Traction current
Ia	Substation A bus instantaneous current
Ib	Substation B bus instantaneous current
I_{fault}	Fault current
Ia_{fault}	Fault current supplied by substation A bus
Ib_{fault}	Fault current supplied by substation B bus
cat	Catenary wire
r_{cat}	Catenary wire resistance
r_{is}	Contact line resistance
Ia^{nth}	Instantaneous current supplied by Substation A bus at the nth coordinate
Ib^{nth}	Instantaneous current supplied by Substation B bus at the nth coordinate
n^{th}	n^{th} network coordinate
zs	Contact line impedance
n	Network coordinate
con	Contact wire
r_{con}	Contact wire resistance
fe	Feeder wire
r_{fe}	Feeder wire resistance
z	Per unit impedance of line
pu	Per unit

II. 3 kV DC Current Distribution Concepts

In some railway-based mass-rapid systems, the 3 kV DC electrification network topology comprises the architectural design of tracks incorporating overhead contact lines fed in parallel from adjacent substations with a HSCB unit protection scheme. Each contact line is

Manuscript received August 5, 2021; revised December 28, 2021.

©2022 Int. J. Electron. Electr. Eng.
doi: 10.18178/ijeee.10.1.7-13

protected by de facto HSCBs at each terminal end. The protection design typifies an open zone for island-fed sections with an HSCB at its terminal end; and a closed zone for contact lines protected by HSCBs at each terminal end as elaborated by [1].

The network operates in a condition different from the commercial and industrial enterprise's static electrical load profiles. The difference is in-network loading profiles and characteristics made by overlapping current consumed by moving EMUs electrical loads from the substations. The EMUs network loading is characterized by accelerating, cruising, coasting, regenerative braking, and stopping. The EMUs motion features regular stops and goes as it moves from station to station. While the EMUs-motion power demand could be constant, it creates a traveling wave of a power node that causes power tracking in the network and shifts the current distribution in the lines and load shift in the substations. The loading becomes complex with multiple EMUs in a section.

Ref. [2] gave a significant mathematical methodology for deriving current distribution in traction networks and its influence on current distribution for the traction network with equal substation DC bus voltages $V_a = V_b$, and unequal bus voltages $V_a > V_b$ connected in parallel to the network with the following treatment. (V_a and V_b are taken as references to the substations bus voltages in the study. V_a is substation A, and V_b is substation B bus voltages). We can modify voltage drop calculation equations demonstrated by [3] and come with the similar treatment as presented by [2]. The equations from [2] and [3] emulate real-time current distribution for substation DC buses with equal voltages where $V_a = V_b$ and unequal voltages where $V_a > V_b$ with currents from the substations distributed inversely proportional to the distances from the point of pantograph – contact wire interface. We characterize the case of current distribution where $V_a = V_b$ with these equations. The current tracking characteristic on the network is a time-variant function of an incremental step change Δs in distance s. The current real-time component on the nth ordinate along the line i.e., the instantaneous current I_a from substation A and I_b substation B is expressed by Eq. (1) and Eq. (2) below:

$$Ia^{\mathrm{nth}} = I.(1 - \tfrac{\Delta s}{s}) \quad (1)$$

$$Ib^{\mathrm{nth}} = I \cdot (\tfrac{\Delta s}{s}) \quad (2)$$

Assuming that there is a constant power demand, the instantaneous distribution current expression for current demand per network coordinate I supplied by substation A bus is given by Eq. (3):

$$Ia = I.\left(1 - \tfrac{\Delta s1}{s}\right) + \cdots I.\left(1 - \tfrac{\Delta s2}{s}\right) \ldots + I.(1 - \Delta sn(n+1))/s \quad (3)$$

while Eq. (3) is the expression for the instantaneous current demand distribution current for Substation A bus, the current demand per network coordinate supplied by the substation B bus is given by Eq. (4):

$$Ib = I.\tfrac{\Delta s1}{s} + \ldots Itr.\tfrac{\Delta s2}{s} \ldots + I.\Delta sn(n+1)/s \quad (4)$$

These equations reveal that the load current seen by the substation buses towards each other diminishes in inverse proportion to the distance from either substation.

This current concept applies to fault conditions where the prospective fault current is distributed congruently with (1) and (2) where I_{fault} is the fault current at the n^{th} ordinate along the line is computed from Eq. (5) and Eq. (6):

$$Ia^{\mathrm{nth}} = Ifault.(1 - \tfrac{\Delta s}{s}) \quad (5)$$

$$Ib^{\mathrm{nth}} = Ifault \cdot \Delta s/s \quad (6)$$

A unique feature of the network scheme is found in substations with DC bus voltages at different potentials connected in parallel to the traction network. Consequently, a high asymmetry of the distribution of current occurs. [2] elaborated on this fact while [4] further elaborated with a worked example of the minimum point of potential $\frac{\delta V}{\delta x} = 0$.

The case of substations with buses at different potential imposes loading and protection constraints. As a result, the bus at a higher potential current loading overlaps into the lower potential bus while the lower potential bus diminishes supplies by a lesser load current with a current factor $(V_a\text{-}V_b)/zs$ supplied by the higher potential bus (where z is the resistance/impedance per unit length of the section length). With the difference in potential at the substation nodes, the minimum point of potential along the contact line section is not equidistant from the substations. This is collaborated by the extent of the load reach of the higher potential bus comparable with the lower potential. We characterize the case of current distribution where $V_a > V_b$ with these equations. Again, the current tracking characteristic on the network is a time-variant function of distance and the time current component on the n^{th} ordinate along the line i.e. the instantaneous current is expressed by Eq. (7):

$$Ia^{\mathrm{nth}} = I.(s - \Delta s1)/s + (Va - Vb)/zs \quad (7)$$

The current from the adjacent substation with a lower bus potential is also given by Eq. (8)

$$Ib^{\mathrm{nth}} = I.(\Delta s1)/s - (Va - Vb)/zs \quad (8)$$

Assuming constant power demand, the instantaneous distribution current expression for current demand per network coordinate supplied by the substation with a higher potential bus is given by a series in the form of Eq. (9):

$$Ia = \tfrac{I.(s-\Delta s1)}{s} + \tfrac{(Va-Vb)}{zs} \ldots \ldots . \tfrac{I.(s-\Delta s2)}{s} + \tfrac{(Va-Vb)}{zs} \ldots \tfrac{I.(s-\Delta s(n+1))}{s} + (Va - Vb)/zs \quad (9)$$

The current from the adjacent substation with a lower bus potential is also given by a series also in the form of Eq. (10):

$$Ib = \tfrac{I.\Delta s1}{s} - \tfrac{(Va-Vb)}{zs} \ldots \tfrac{I.\Delta s2}{s} - \tfrac{(Va-Vb)}{zs} \ldots \tfrac{I.\Delta sn(n+1)}{s} + (Va - Vb)/zs \quad (10)$$

For distributed EMUs in the section, the instantaneous distributed current expression for total current demand per EMU coordinate in the network supplied by substation at a higher potential is given by Eq. (11):

$$f(sa) = \mathrm{I} \sum_{s=1}^{s=n+1}((s - \Delta s1)/s) + (Va - Vb)/zs) + (s - \Delta s2)/s) + (Va - Vb)/zs \ldots + (s - \Delta sn(n+1)/zs + (Va - Vb)/zs)) \quad (11)$$

While that supplied by the adjacent substation is shown in Eq. (12):

$$f(sb) = \mathrm{I} \sum_{s=1}^{s=n+1}((s\Delta s1)/s) - (Va - \mathrm{V}b)/zs) + ((s\Delta s2)/s) - (Va - Vb)/zs)) + \cdots (z\Delta s(n=1)/s) - (Va - Vb)/zs)) \quad (12)$$

In faults and fault currents, the same argument follows and presents a critical state for the HSCB unit protection scheme. The scenario gets worsened by high impedance or resistance faults that may occur below the intrinsic breaker set values. It is not feasible within the network configuration to implement any form of a protection scheme with the use of HSCBs only. Nonetheless, the network configuration is a closed zone and protection and coordination can be employed.

In the simulation computations, it is assumed that the contact line parameters remain constant. We treat concept's analysis with simplicity i.e., current distribution for the traction network with equal substation DC bus voltages $V_a = V_b$. In the 3 kV DC application, adjacent traction substations are cascaded to feed the same contact line sections in parallel with breakers at its terminal ends. For protection, it is the practice to use the same overcurrent breaker setting threshold on breakers to detect faults. When faults occur, abnormal currents flow and trigger breakers to trip. Based on the traction network current distribution, and breakers as stand-alone units HSCB tripping is independent of each other when clearing faults, i.e., the breaker that is closer to an overload or a fault trips, while the one that is at the remote end does not trip or takes time to trip. Under these conditions, the breaker that does not trip or delays tripping keeps supplying residual current into a fault.

While breakers can successfully clear faults, and with islanded electronic control relays mounted on breaker trolleys or cells for control, electronic control relays independently recover supply by auto reclose. In contrast, while line faults have not cleared, i.e., electronic control relays independently close the HSCBs they are assigned to "uninformed" and without coordination. The relays have no capability of integration to synchronize and coordinate breakers operation under fault conditions. From a 3 kV DC network management perspective, though HSCBs could successfully clear faults with a lockout, control officers can reset and reclose breakers by telemetry unaware of network status. The system cannot manage the network. With the advent of digital devices, the challenge remains as the devices are implemented as uncoordinated and none-integrated stand-alone units.

III. Modelling

Determination of conductors' thermal characteristics is complex. Several variables, particularly environmental factors and meteorological conditions, critically influence the conductivity of conductor materials at any given ambient temperature as detailed in [5] and [6]. For consistency, the conductors' material constants are taken at 20° C to eliminate the complexities of creating algorithms for tracking and calculating compensation factors required for changes in conductors' constants exposed to varying conditions mentioned in the standards.

The substations configurations with the resultant capacities and constants are demonstrated by [7]; with the related contact line constants are used to derive fault current level per network coordinate. While Infrastructure managers do not include rail inductance constants in their standards for short circuit calculation, [8] detailed the analysis of appropriate electrical impedance models for steel railway rails suitable for power supply transient fault calculations. In an $r + jx$ inductive circuit, an AC short-circuit current comprises decaying AC and decaying DC components. Contrary to DC systems short circuit calculations, inductance is often ignored. In DC contact line systems, steel rails are used as return conductors. Based on [9], steel rail inductance is going to be adopted and assumed to moderate the time constant of the network as clarified by [10] and [11].

The contact line profile is made up of

- 161 mm^2 hard-drawn grooved copper contact wire (con) with its resistance stipulated in BS EN 50149 (2012)
- 80 mm^2 hard-drawn copper stranded catenary wire (cat) with its resistance stipulated in SANS 182-1 (2008)
- 500 mm^2 stranded aluminium feeder wire (fe) with its resistance stipulated in IEC-SANS 182-2 (2008).

The resistance of the conductors is at an ambient temperature of 20°C. The resistance of a 3 kV DC contact line with the parallel conductors is given per unit length given by

$$\mathrm{r}_{\mathrm{is}} = \sum_{r=1}^{n} 1/r^n$$

and for the three contact line conductor profile

$$1/\mathrm{r}_{\mathrm{is}} = 1/\mathrm{r}_{\mathrm{cat}} + 1/\mathrm{r}_{\mathrm{fe}} + 1/\mathrm{r}_{\mathrm{con}}$$

$$\mathrm{r}_{\mathrm{is}} = (\mathrm{r}_{\mathrm{cat}} . \mathrm{r}_{\mathrm{fe}} . \mathrm{r}_{\mathrm{con}})/((\mathrm{r}_{\mathrm{cat}} . \mathrm{r}_{\mathrm{fe}}) + (\mathrm{r}_{\mathrm{fe}} . \mathrm{r}_{\mathrm{con}}) + (\mathrm{r}_{\mathrm{con}} . \mathrm{r}_{\mathrm{cat}})) \quad (13)$$

Furthermore, the ampacity of the contact line is the sum of the current flowing through each of the conductors and is given by

$$\mathrm{I} = \mathrm{I}_{\mathrm{cat}} + \mathrm{I}_{\mathrm{fe}} + \mathrm{I}_{\mathrm{con}} \quad (14)$$

The current is dependent on the impedance/resistance of the individual conductor. Therefore, the current flowing through the contact wire Ir_{con} is

$$\mathrm{Ir}_{\mathrm{con}} = \mathrm{I}.(\frac{\mathrm{r}_{\mathrm{is}}}{\mathrm{r}_{\mathrm{con}}}) \quad (15)$$

The current flowing through the catenary wire Ir_{cat} is

$$Ircat = I.(\frac{ris}{rcat}) \quad (16)$$

and the current flowing through the feeder wire I_{fe} is

$$I_{fe} = I.(\frac{ris}{rfe}) \quad (17)$$

As stated by [3], the ampacity of the contact line I is determined by the conductor that first reaches its thermal limit. Corollary, that conductor should be protected from thermal run away by the protection scheme.

The mathematical model, i.e., the Fourier transform of the exponential impulse equation of short circuit response is run on the MATLAB. The data collated from the line constants are formatted in the current distribution equations and converted to the algorithms that manipulate the data in a simulation of the selected line coordinates that output results useable for graphical analysis.

IV. Simulation

This paper presents results from the MATLAB/Simulink models and simulations to explore the limitations in HSCB unit protection scheme. First, the HSCB unit protection is evaluated based on Eq. (3), Eq. (4), Eq. (5) and Eq. (6) on the phenomena of fault current level distribution along the contact line. Then, HSCB unit protection coordinated tripping with a peer-to-peer direct transfer tripping scheme as an end-to-end protection solution is explored with high impedance faults, and on the extant of the limitation on the 3 kV DC power system protections as depicted in Fig. 1 below.

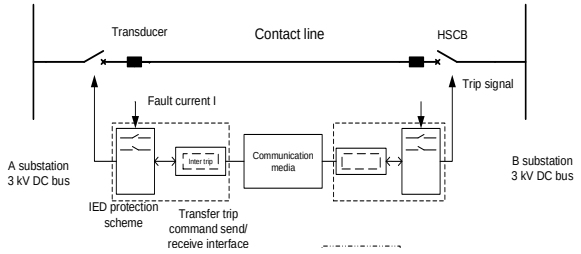

Figure 1. HSCB unit protection with a peer-to-peer direct transfer tripping scheme.

V. Results Analysis and Discussion

The fault current for the design matrix of the substation switching configuration with the resultant contact line fault current level distribution is shown Fig. 2.

The protection indecisive responses for high impedance faults on the of the protection scheme with and without telemetry are shown in Fig. 3-Fig. 7 for both different input variables and fault locations. The responses properties are discussed in the proceeding sections.

Fig. 3 below shows the performance of the protection scheme without telemetry. At any given time, only one breaker is insensitive to the faults occurring in that part of the contact line section with infinite dead time. The other breaker detects the fault that is within its reach.

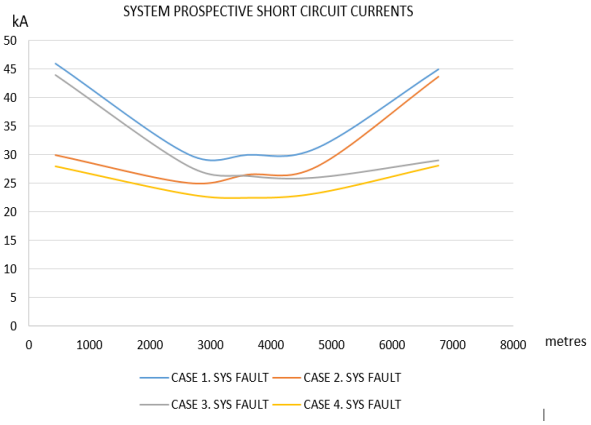

Figure 2. Fault level current distribution for: Case 1 20MVA, Case 2 15 MVA, Case 3 15 MVA and Case 4 10 MVA network capacities.

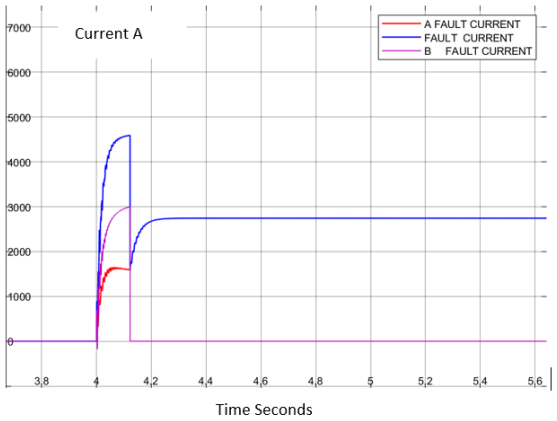

Figure 3. Overall fault current in a HSCB unit protection scheme high impedance fault clearance without telemetry (Residual current fed by substation A during a fault clearance).

Fig. 4 below shows the protection scheme performance for a remote fault where the fault current magnitude is insufficiently high such that the HSCBs cannot detect the fault current and continue to supply energy into the fault. HSCB calibration for protection setting sensitivity at each end of the contact line cannot (be set to) cover the whole length of the contact line. Where faults occur outside the precincts of the substations, they are out of reach of protection.

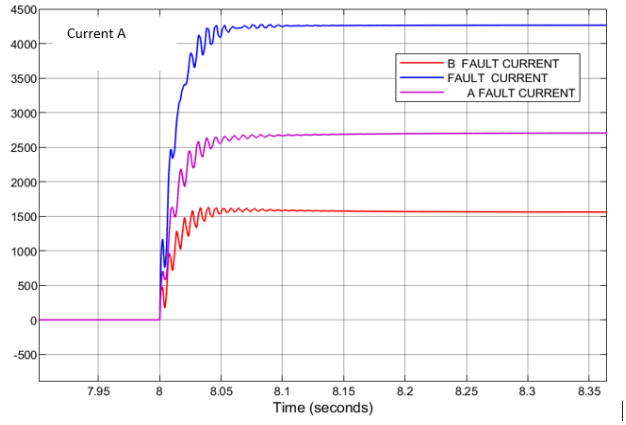

Figure 4. HSCB unit protection scheme distant high impedance fault clearance performance with and without telemetry.

Fig. 5 shows the performance of the protection scheme for remote end high impedance fault clearance performance with and telemetry. The protection at either end of the line positively detects the fault and provides a high-speed inter-tripping signal. This results in both breakers tripping instantaneously and in synchronism.

Fig. 6 and Fig. 7 show the detailed fault clearance performance from Fig. 3. In Fig. 6 below, the contact line conductors' current profiles of the residual fault current distribution fed by Substation A into contact line section. The overall fault current at the point of fault is lesser than the HSCB protection trip setting value.

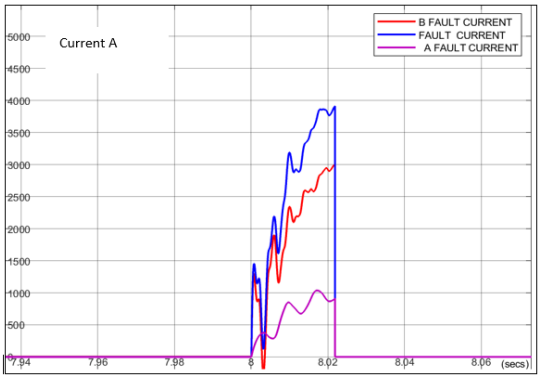

Figure 5. HSCB unit protection scheme remote end high impedance fault clearance performance with and telemetry.

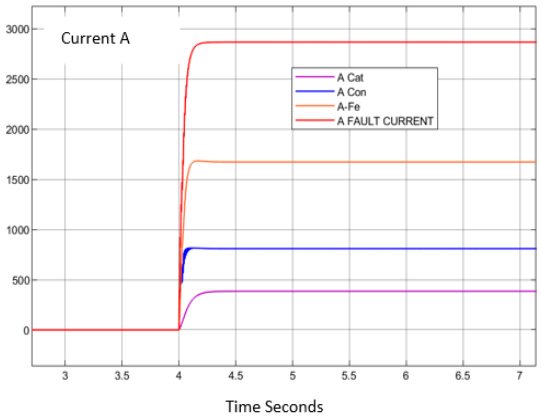

Figure 6. Residual fault current distribution in conductors fed by Substation A into contact line section.

Fig. 7 details the transient time stamp on the breaker tripping and duration of exposure of the contact line conductors to network faults and fault current peaking in the individual conductors at substation B.

Table 1 below shows the stead state remnant fault current impressed on the contact line conductors from Fig. 6 statistics.

TABLE I. CONDUCTOR RATINGS AND OBSERVED REMNANT FAULT CURRENT

	Ratings		Observed remnant fault current Refer to Fig. 6
	Continuous	5 minutes	
Catenary Wire (Cat)	366 A	470 A	384,8 A
Contact Wire (Con)	586 A	986 A	822,9 A
Feeder Wire (Fe)	887 A	1894 A	1683 A

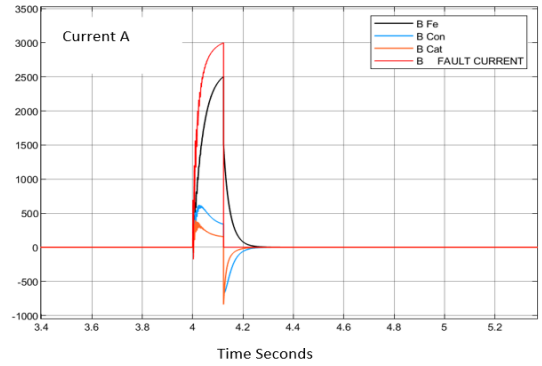

Figure 7. Conductors current profiles during circuit breaker fault clearance by Substation B.

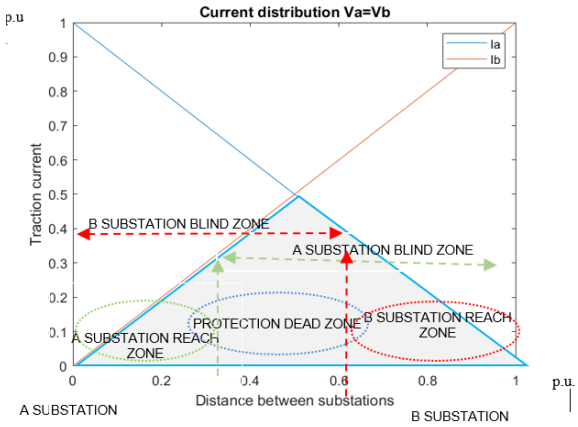

Figure 8. HSCB unit protection scheme protection zones.

Based on the specifications, Table 1. shows the ratings of the conductors in columns 1 and 2. Column 3 shows the observed conductor loading for a high impedance fault with the sustained fault currents. The currents are above the maximum mean loading of the conductor continuous ratings and well above their thermal load capacity. The resultant is the compromise of the rectifier equipment's thermal limit. The conductors' temperature elevates, resulting in the impairment of the mechanical properties of the conductors. The HSCB does not protect the conductor that reaches its thermal limit first, but collectively protects the three conductors compromising that conductor reaching its thermal limit first.

In Fig. 6. Substation A breaker does not trip because the fault current magnitude is insignificantly low below its threshold setting. The breaker cannot detect the fault current and continues supplying energy into the fault. Contrary to Fig. 6 substation A, Fig. 7 substation B HSCB, due to its proximity to the fault senses, trips, and clears the fault. An exception lies in the midsection where both breakers do not sense the fault, as in Fig. 4. The contact line section is exposed to fault current in-feeds from both ends. Protection decisiveness is not achieved and is self-conflicted. The breaker that does not sense the fault continues as a source of energy, supplying energy into the fault. The HSCB calibration setting sensitivity at one end of the line cannot cover the length of the contact line. At any given time, only one breaker is insensitive to the faults in that part of the contact line infinite dead time.

©2022 Int. J. Electron. Electr. Eng.

Fig. 5 shows HSCB unit protection scheme remote end high impedance fault clearance performance with telemetry. The exception is in the midsection, where both breakers do not sense the fault, as shown in Fig. 4. Since the teleprotection depends on the feedback of relay trip signal, it is of no effect.

HSCB protection settings are calculated to ensure the clearance of track - contact lines short circuits and not EMUs faults or fault impedances less than their dynamic impedances. Fig. 8. summarizes the results of the areas of protection zones formed in the HSCB unit protection scheme. During high impedance faults, the rate of rise and fault current levels at the points of fault is lesser at either of the substations. The overall fault current at the points of fault as we traverse away from either substation continually falls to a lesser value than the HSCB trip setting value. Therefore, the probability of mal-operation is prevalent. Fig. 3, Fig. 6 and Fig. 7 are fault phenomena.

The scheme cannot protect the entire contact line section with certainty. This concurs with the findings of [12] and [13] with respect to HSCBs that their performance does not comply with the EN 50123 2 specifications.

Prospective short circuit currents protection is catered for by the breaker intrinsic trip setting that is set as back-up; or by the intelligent devices rate of rise of current threshold when the gradient of the fault current lies outside the EMUs slope of the traction current load line. When the gradient of the fault current lies within the EMUs slope of the traction current load line, the rate of rise of current detection is not certain.

With EMUs' start-up, the starting current reaches a maximum value and reduces gradually within a specific time interval. Though the maximum values of the starting current in the EMUs and the fault current are comparable, the fault current increases instantaneously, reaching a maximum and sustains that maximum value unless interrupted, whereas the starting current requires a specific time to reach a maximum value, and then drops to a minimum value. These characteristics can be used to formulate algorithms to discriminate the EMUs starting current from high impedance faults and critical fault current of significantly low magnitudes.

VI. Conclusion

The HSCB unit protection scheme is ideal for short circuit protection. The use of the HSCB unit protection scheme for other faults protection leads to a large blind zones and their overlaps in the contact line section in between the substations where high impedance faults are of concern as explained by Fig. 4, Fig. 5 and Fig. 7. It is not feasible to define the sensitivity for zone protection, let alone the (blind) zone reach compensation. Neither is it practical to define the dead zone on the contact line section as there is no flexible methodology calculating and selecting the settings. This compromises the reliability of the protection scheme and the security of the power supply. (The dead zone is that portion of the contact line section whereby the protection scheme is not capable of selectively discriminating the faults. There is incomplete protection coverage). [14], [15] and [16] presented similar works on the effectiveness of the rate of rise of current and current increment protection attributes of the product (i.e., relay) rather than a protection scheme. Comparatively, other than the effectiveness of the rate of rise protection on the unit scheme, there are constraints in the studies on the protection coordination and its implement ability as a holistic protection scheme with real-time communication systems.

The transfer trip concept with the rate of rise protection minimizes the risks on protection limitation on the exclusion of the dead zone where the protection of one HSCB overlaps the protection of the other breaker by use of IEDs which are communication capable. The concept is the heartbeat of relay logic status real-time communication between devices. The rate of rise of current protection augmented with the transfer trip scheme is an optimum end-to-end strategy to fully idealise the HSCB unit protection scheme for a total 3 kV DC contact line protection.

Conflict of Interest

The authors declare no conflict of interest.

Author Contributions

Wonder Mukwata conducted the research using MATLAB modelling, simulation, data collation, and analysis. Josiah Munda reviewed the scripts and approved the final version.

Acknowledgment

The authors wish to thank the Tshwane University of Technology, Department of Electrical Engineering, Faculty of Engineering and the Built Environment for providing the necessary resources in the computer laboratory. They also extend their gratitude to the support staff for their collaboration during the research.

References

[1] M. Wang, M. Abedrabo, W. Leterme, D. V. Hertem, C. Spallarossa, S. Oukallia, L. Grammatikos, and K. Kuroda, "A review of AC and DC protection equipment technologies: Towards a multivendor solution," *Cigré Winnipeg, Colloquium Study Committees A3, B4 & D1, Cigre, B4-047*, 2017.

[2] V. Sopov, E. Abramov, N. Schurov, and E. Langeman, "Traction network currents distribution under different power supply voltage," *Advances in Engineering Research*, vol. 133, 2017.

[3] F. Kiessling, R. Puschmann, A. Schmieder, and E. Scheider, *Contact Lines for Electric Railways: Planning, Design, Implementation, Maintenance*, 3rd ed., Erlangen, Germany: Publicis Publishing, 2018, ch. 5, pp. 298-300.

[4] M. Soni, P. Gupta, and U. Bhatnagar, *A Course in Electrical Power*, Nai Sarak Delhi: Dhanpat Rai and Sons, 1991, Part 2, ch. 8, Example 8.8, p. 155.

[5] L. Staszewski and W. Rebizant, "The differences between IEEE and CIGRE heat balance concepts for line ampacity considerations," in *Proc. International Symposium on Modern Electric Power Systems*, 2010, pp. 1-4.

[6] IEEE Standard for Calculating the Current-Temperature Relationship of Bare Overhead Conductors, IEEE Std 738-2012 (Revision of IEEE Std 738-2006 - Incorporates IEEE Std 738-2012 Cor 1-2013), 23 Dec. 2013.

[7] J. Read, "The calculation of rectifier and inverter performance characteristics," *Journal of the Institution of Electrical Engineers-Part II: Power Engineering*, vol. 92, no. 29, pp. 495-509, 1945.
[8] J. Brown, J. Allan, and B. Mellitt, "Calculation of remote short circuit fault currents for DC railways," *IEE Proceedings B Electric Power Applications*, vol. 139, no. 4, pp. 289-294, 1992.
[9] J. Brown, J. Allan, and B. Mellitt, "Calculation and measurement of rail impedances applicable to remote short circuit fault currents," *IEE Proceedings B Electric Power Applications*, vol. 139, no. 4, pp. 295-302, 1992.
[10] P. Silvester, "Modal network theory of skin effect in flat conductors," *Proceedings of the IEEE*, vol. 54, no. 9, pp. 1147-1151, 1966.
[11] P. Silvester, "The accurate calculation of skin effect in conductors of complicated shape," in *IEEE Transactions on Power Apparatus and Systems*, vol. PAS-87, no. 3, pp. 735-742, March 1968.
[12] A. Rojek, "Parameters of DC high-speed circuit breakers," in *Proc. 13th International Conference Modern Electrified Transport*, vol. 180, 2018.
[13] A. Rojek and M. Siderowicz, "Researches and tests of high speed circuit breakers for rolling stock and substations in 3 kV DC traction power systems," *Problemy Kolejnictwa*, vol. 159, pp. 7-30, 2013.
[14] E. Cinieri, S. Cosmi, A. Fumi, V. Salvatori, and W. Torto, "A new digital protection of the 3 kV DC electric traction lines, Results of the Application of Four Prototypes in Italy," thesis, University of L' Aquila, Italy, 2020.
[15] M. X. Li, J. H. He, Z. Q. Bo, H. T. Yip, L. Yu, and A. Klimek, "Simulation and algorithm development of protection scheme in DC traction system," in *Proc. 2009 IEEE Bucharest PowerTech*, 2009, pp. 1-6.
[16] M. T. Hagh, B. Nouri, M. Nouri, H. Lomei, and K. M. Muttaqi, "A new protection scheme for the DC traction system supply," in *Proc. 2015 Australasian Universities Power Engineering Conference*, 2015, pp. 1-6.

Copyright © 2022 by the authors. This is an open access article distributed under the Creative Commons Attribution License (CC BY-NC-ND 4.0), which permits use, distribution and reproduction in any medium, provided that the article is properly cited, the use is non-commercial and no modifications or adaptations are made.

Wonder Mukwata is an Electrical Specialist employed by Metrorail. He works in the Electrical Department on roles overseeing the 3kV DC traction power supplies and 11kV and 33kV AC primary power supplies for the traction substations. He is actively involved in the research and product development on the concepts and acceptance of the introduction of Feeder Protection Relay as product solutions and their conversion to protection solutions for the 3kV DC traction power supplies. He had extensive exposure to the 25kV traction power supplies with the National Railways of Zimbabwe. He has a Bachelor of Technology degree from the University of South Africa and is currently reading for a Master's Degree in Engineering with the Tshwane University of Technology in Pretoria.

Josiah Lange Munda received the MSc degree in electric power supply from Tver State Technical University in 1991 and the DEng degree in electrical engineering from the University of the Ryukyus in 2002. He is currently a Professor of electrical engineering, and the Assistant Dean of postgraduate studies, research, and innovation with the Tshwane University of Technology, South Africa. He has authored or coauthored more than 200 articles in peer-reviewed journals, book chapters, and international conference proceedings and journals. His main research interests include power system analysis, energy efficiency, and demand-side management and microgrids. He is a Member of IEEE and a Senior Member of the South African Institute of Electrical Engineering.